Iranian Journal of Medical Physics

ijmp.mums.ac.ir

# Consideration of Individual Brain Geometry and Anisotropy on the Effect of tDCS

Mohsen Mosayebi Samani[1], Seyed Mohamad Firoozabadi[2*], Hamed Ekhtiari[3]

[1] Department of Biomedical Engineering, Tarbiat Modares University, Tehran, Iran.
[2] Department of Medical Physics, Tarbiat Modares University, Tehran, Iran.
[3] Neurocognitive Laboratory, Iranian National Center for Addiction Studies (INCAS), Tehran University of Medical Sciences, Tehran, Iran.

**ARTICLE INFO**

***Article type:***
Original Article

***Article history:***
Received: Mar 01, 2017
Accepted: May 22, 2017

***Keywords:***
Brain
Finite Element
Individual Difference
tDCS

**ABSTRACT**

***Introduction***: The response variability between subjects, which is one of the fundamental challenges facing transcranial direct current stimulation (tDCS), can be investigated by understanding how the current is distributed through the brain. This understanding can be obtained by means of computational methods utilizing finite element (FE) models.

***Materials and Methods:*** In this study, the effect of realistic geometry and white matter anisotropy on the head electrical current density intensity (CDI) distribution was measured using a magnetic resonance imaging (MRI)-derived FE model at the whole brain, below electrodes, and cellular levels.

***Results:*** The results revealed that on average, the real geometry changes the CDI in gray matter and the WM by 29% and 55%, respectively. In addition, WM anisotropy led to an 8% and 36% change of CDI across GM and WM, respectively. The results indicated that for this electrode configuration, the maximum CDI occurs not below the electrode, but somewhere between the electrodes, and its locus varies greatly between individuals. In addition, by investigating the effect of current density components on cellular excitability, significant individual differences in the level of excitability were detected.

***Conclusion:*** Accordingly, consideration of the real geometry in computational modeling is vital. In addition, WM anisotropy does not significantly influence the CDI on the gray matter surface, however, it alters the CDI inside the brain; therefore, it can be taken into account, especially, when stimulation of brain's internal regions is proposed. Finally, to predict the outcome result of tDCS, the examination of its effect at the cellular level is of great importance.

► *Please cite this article as:*
Mosayebi Samani M, Firoozabadi SM, Ekhtiari H. Consideration of Individual Brain Geometry and Anisotropy on the Effect of tDCS. Iran J Med Phys 2017; 14: 203-218. 10.22038/ijmp.2017.22243.1209.

## Introduction

Transcranial direct current stimulation (tDCS) is a non-invasive and painless stimulation method, which induces desirable cortical plasticity in a specific brain region by modulating neuronal excitability [1]. Changes in neuronal excitability conventionally increase or decrease when an anodal or cathodal stimulation is applied, respectively [1, 2]. In addition to current polarity, there are other important factors affecting the response to tDCS, including the electrode configuration, size [3, 4] and current intensity [5].

Despite some unknown physiological mechanisms, tDCS is a promising treatment approach for a wide variety of brain disorders, including Alzheimer's disease [6, 7], Parkinson's disease [8, 9], stroke [10, 11], depression [12, 13], chronic pains [14], as well as cigarette [15] and food cravings [16]. However, one of the barriers to the widespread uptake of tDCS is the fact that the results of similar tests have demonstrated that the effects of this type of stimulation differ between individuals [17]. This is due to several factors, including the brain state [18], age, gender, brain geometrical structure [19, 20], and specific electrical specifications of the brain tissues in each individual [21].

In this regard, in order to examine the effect of tDCS, Wiethoff et al. [22] applied a current of 2 mA to the motor cortex of 53 healthy subjects for 10 min using electrode size of 35 $cm^2$. They applied transcranial magnetic stimulation to measure the amount of corticospinal excitability by the changes of motor evoked potentials to evaluate the after-effects of tDCS. Based on a cluster analysis, they reported that 50% of the individuals had only a minor response or did not respond at all, while the other subjects responded as expected.

Furthermore, with the purpose of measuring the motor evoked potential index, Alonso et al. [23] investigated the effect of applying 1 mA to the motor cortex (M1) of 56 subjects for 13 min on the changes of cellular excitability. The results of the test showed that only 45% of the subjects had the expected response to this type of stimulation. There are

*Corresponding Author: Department of Medical Physics, Tarbiat Modares University, Tehran, Iran. Tel: +98 21 82883821, E-mail: pourmir@modares.ac.ir

different physiological and psychological factors that can confound the tDCS results, including attention, background muscle activity, and muscle fatigue. Out of these factors, the recent studies have drawn special attention to the intra-subject consistency and reliability of response to tDCS.

In this regard, Dyke et al. [24] used transcranial magnetic stimulation recruitment curve to measure the changes in cortical excitability after applying 2 mA anodal, cathodal, and sham tDCS over the motor cortex for 20 min. They found that the anodal tDCS significantly increased the cortical excitability at a group level, whereas cathodal tDCS failed to have any significant effects in this regard. Their results showed that the anodal and cathodal tDCS exhibited poor reliability at an individual level. A recent meta-analysis of tDCS studies also highlighted that the probabilities of achieving the classical "anodal-facilitatory/cathodal-inhibitory" effect on motor and cognitive outcomes were only 0.67 and 0.16, respectively [25].

Given the variation and complexity of the factors affecting the outcomes, it is very difficult to simultaneously measure or examine the independent roles of each factor in the creation of different responses. In addition, the direct measurement of electrical current in a person's brain is complex and carries an element of risk. The intensity and direction of the electrical field applied to a cell is the main factor in changing the cell excitability [26]. Furthermore, the geometry and physics of the brain tissues are the main factors affecting the change in size and direction of electrical field distribution in the brain [27]. Regarding this, a better understanding of the creation of response variability can be obtained by modeling the electrical current distribution in the brain.

Prior to the introduction of the numerical solution methods to calculate the brain current distribution, the analytical methods were utilized [28]. However, in the analytical methods, the structural complexity is not extensible, and the electrodes are normally considered as points, even though differently shaped electrodes can have different effects [29]. Currently, a standard modeling method, which is based on numerical solutions, is used for the calculation of the brain electrical current distribution [27].

In order to examine the brain current distribution, Salvador et al. [30] designed a three-dimensional (3D) model of head geometry extracted from the magnetic resonance imaging (MRI), including scalp, skull, cerebrospinal fluid (CSF), and gray and white matter. Cylindrical anode and cathode electrodes were used and a current of 1 mA was applied to the anode. The results of the simulation indicated that in contrast to analytical modeling results, which predicted that the maximum current density was on gyri close to the electrode, the maximum density was located at a point in the sulci.

In addition, in the mentioned study, it was shown that the changes in the skull electrical conductivity had a major effect on the change of the electrical current magnitude, but a lesser effect on changes of the distribution. Furthermore, the results demonstrated that the changes in the skull and CSF electrical conductivity modified the size and distribution of the electrical current to a great extent. As a result, it is of critical importance to select a suitable electrical conductivity for each subject. However, in the mentioned study, the brain tissues were assumed to be isotropic, which was contrary to reality.

In another study, Data et al. [27] used a new electrode configuration (i.e., ring electrode) to increase the focality of the electrical current. The results of the modeling revealed that the new electrode configuration focalized the current below the electrode in the desired region. However, as brain tissues were assumed to be isotropic in the mentioned study, and the whole brain (i.e., white and gray matter) was considered as one single type of brain tissue, the accuracy of the modeling was reduced.

In addition, Suh et al. [31] investigated the effect of anisotropy of the skull and white matter on the current focalization using a 3D model of the head and finite element (FE) analysis. They demonstrated that taking into account the anisotropy of the brain tissue significantly reduced the current focalization in the ring electrode configuration [27].

There are different anatomical features that influence the current distribution, such as skull thickness [32], subcutaneous fat [20], gyral pattern [33], and orientation of neurons [34]. In a recent study, among these features, CSF thickness was highlighted as a primary factor affecting an individual's electric field [35]. In the mentioned study, the researchers used a MRI finite-element method to computationally estimate the current distribution through the brain of 24 healthy subjects during the tDCS of motor cortex.

In the mentioned study, a group-level statistical analysis on the surface-based inter-subject registration of the electric field and functional MRI data showed that the distance of the hand motor area (HMA) to the inner boundary of the skull was the most important single factor affecting the calculated electric fields. They reported that this factor explained about one-half of the variations in the subject-specific electric fields. This distance was related to the thickness of the CSF, and it was determined by both the total volume of the CSF and the individual cortical morphology of the HMA. They

concluded that a thicker layer of CSF above the HMA resulted in a weaker electric field.

Shahid et al. [36] investigated the effect of brain tissue anisotropic conductivity on changing of brain current distribution. They reported that the application of anisotropy to the model did not lead to any significant changes in the current distribution on the cerebral cortex and was only effective in the electrical current intensity. Therefore, considering anisotropy when determining the electrical current intensity and distribution in clinical applications only complicates the model and increases the cost of model generation.

However, the results of another study [37] showed that although the application of white matter anisotropy resulted in small changes in the electrical current distribution and intensity on the cortical layer, it greatly altered the spatial distribution of the current density intensity (CDI) inside the brain. Regarding this, they suggested that the consideration of anisotropy is essential to increase the safety and efficiency of tDCS.

In line with the effect of anisotropic brain tissue property on the whole brain current distribution, Metwally et al. [38] investigated the effects of the skull and white matter anisotropy on the radial and tangential components of the electric field via high-resolution finite element head models. It was found that the skull anisotropy had a crucial impact on the distribution of the radial electric field component and white matter anisotropy strongly altered the electric field directionality, especially within the sulci.

To the best of our knowledge, studies investigating the effect of one important factor, such as brain geometry or anisotropic conductivity, on changing of the brain current distribution have generally focused on one subject. Furthermore, the effects of anisotropy are generally measured by approximate equations, which are the same for all models. On the other hand, the results of these studies are limited to the measurements of current intensity, and the effect of current direction is not well investigated. In this context, there is a strong need to investigate the effects of brain geometry and anisotropic conductivity on current intensity and direction at the whole brain, region of interest, and cellular levels.

In the present study, we measured and simulated the relationship between the effects of tDCS and the specific features of the individual using a 3D computer model of a human head based on MR images. To this aim, the brain geometry was first recovered using MR images, and average values for electrical conductivity of the brain tissues were obtained from the literature. After adding the anisotropic feature of the electrical conductivity of the brain tissues, which was extracted from the diffusion tensor (DT) images, the brain current distribution was calculated using the numerical solution method and the quasi-static approximation.

In the analysis of the results, the effect of the geometry and anisotropy of the brain tissues on the changing of the electrical current distribution across the gray matter, white matter, and below the electrodes at the cortical layer was evaluated. In addition, the electrical current distribution in a neuron, together with the effect of the distribution on the cell excitability, was discussed and investigated, taking into account the dominant direction of the electrical current at the point for each person.

## Materials and Methods

The current distribution in the head was calculated using the MRI and DT images of four subjects, through the SPM8 software package (Welcome Trust Center for Neuroimaging, London, UK) to segment the head elements into five sections, namely skin, skull, CSF, gray matter, and white matter (Figure 1). In the next step, a 3D model, including the geometry of the head and electrodes, was built using the Simpleware version 3.1 (Synopsys, Mountain View, USA). Subsequently, the anisotropy features of the brain tissues were measured based on the extracted diffusion tensor using the FSL (Functional MRI of the Brain Software Library, United Kingdom) software.

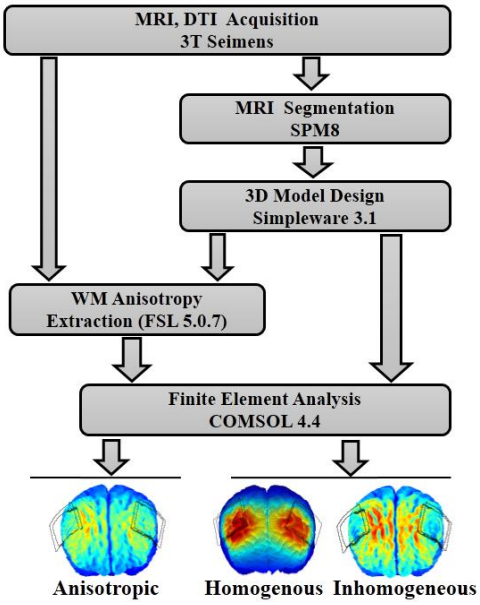


**Figure 1.** Workflow of designed study. After acquiring MRI and DTI images of four subjects, software package SPM8 was used to segment the head elements. Then, a three dimensional model was built using Simpleware v.3.1, and the anisotropy feature of the brain were measured based on the extracted diffusion tensor using FSL. Finally, the current distribution was calculated using the numerical solution method in COMSOL v.4.1 for the case of homogeneous, inhomogeneous and anisotropic model.

Finally, after entering the designed 3D model into the COMSOL Multiphysics software package version 4.1 (COMSOL, Inc., Burlington, MA), the current distribution in the head was obtained. In the analysis of the results, we evaluated the effect of the realistic geometry and white matter anisotropy on the change of size and distribution of electrical current across the gray matter, white matter, and below the electrodes at the cortical layer.

To analyze the effects of geometry, a homogeneous and inhomogeneous realistic head model was built and the current distributions were compared to each other. Furthermore, in order to investigate the effect of white matter anisotropy on the change of the head current intensity and distribution, the current distribution was calculated assuming white matter anisotropy, and the results were then compared with the isotropic case.

**Magnetic Resonance Imaging And Diffusion Tensor Imaging Data Acquisition**

The anatomical T1-weighted MRIs and DT images of four healthy subjects (male, 29.5±1.3)were obtained on a Siemens 3T MRI scanner (Siemens, Erlangen, Germany). T1-weighted coronal MRI images were acquired using a fast spin-echo sequence (repetition time [TR]=1800 ms, echo time [TE]=3.44 ms, 256×256 image matrix with 176 slices, 1×1×1 $mm^3$ voxel). The diffusion images were obtained using a cardiac-gated pulsed gradient sequence with the echo planar readout (TR=12,000 ms, TE=90 ms, slice thickness=2 mm, image matrix=256×256) and the diffusion sensitizing gradients with a b-value of 1,000 $s/mm^2$.

***Realistic Three-Dimensional Head Model Generation***

First, the raw images, which were saved in the DICOM format, were converted to the NIFTI format using the MRICRO software package (Center for Advanced Brain Imaging, Atlanta, USA). Then, the automatic algorithm of SPM8 was used to segment the image into four regions, namely skull, CSF, gray matter, and white matter (Figure 2). In order to build a 3D model of the segmented images of each person, the manual segmentation tools in the ScanIP software package (Synopsys, Mountain View, USA) were employed. Subsequently, the stimulation of the electrodes (25 $cm^2$) as well as the gel between the electrode and scalp was made and added to the model using the ScanCAD software package (Synopsys, Mountain View, USA).

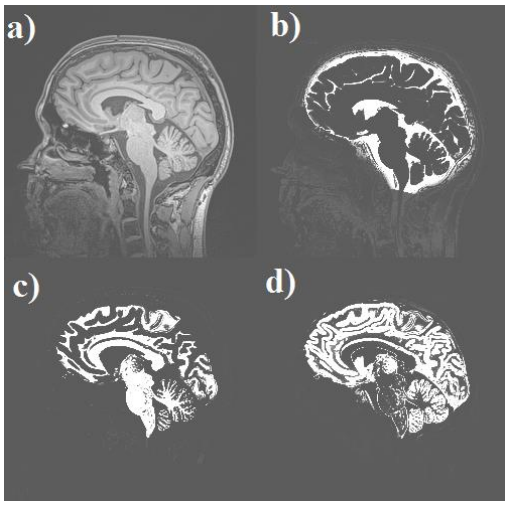


**Figure 2.** Example of segmented key tissues: a) MR image without segmentation; b) segmented cerebrospinal fluid; c) segmented White matter; and d) segmented Gray matter. All images are correspond to MR slice number 82 of 176.

The locations of the electrodes were chosen based on the international 10-20 system for the electroencephalography electrode placement. Accordingly, the anode and cathode electrodes were placed on F4 and F3, respectively. Then, the mesh model was formed using the ScanFE software package (Synopsys, Mountain View, USA), and the appropriate output was obtained for processing by means of the COMSOL Multiphysics software package version 4.1. Overall, the final model comprised 18 million tetrahedral meshes (Figure 3).

Because of the noise in the MRI images, the image segmentation methods always contain minor errors [39], including discontinuities in the CSF, disconnected voxels, unassigned voxels, and rough tissue masks (Figure 4). To reduce those errors, we used manual segmentation tools, such as paint and threshold as well as morphological tools such as dilate/erode and recursive Gaussian smoothing filter in the ScanIP software package.

In order to increase the accuracy and adaptability of the model and segmented images, the segmented MR images were used as a background of the binary images in all stages. The elimination of such errors is normally performed manually, which is very time consuming. In a new study, an automatic algorithm was proposed to eliminate these errors [39], which could increase the accuracy and design speed of the model and could be considered in future studies.

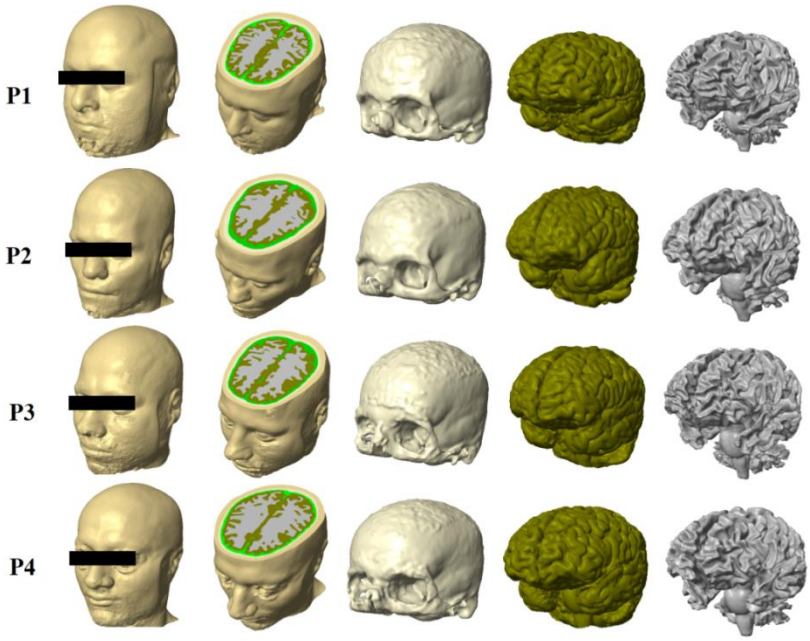


**Figure 3.** 3D realistic head model of four subjects P1-P4 based on segmented MR images and consists of five tissue compartment models (skin, skull, cerebral spinal fluid (CSF), gray matter and white matter).

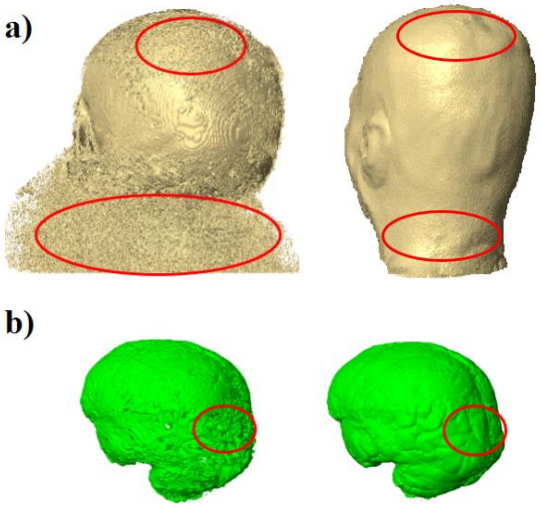


**Figure 4.** Examples showing errors in the segmentated images from SPM8 and the improvements after corrections by manual segentation tools in ScanIP, as indicated by red circles. (a) "disconnected" voxels and rough tissue surface (b) discontinuities in CSF.

### *Determination of Electrical Conductivity Properties of Brain Tissues*

Taking into account the low frequency (0-10 kHz) of transcranial brain electrical stimulation, the quasi-static approximation can be used to measure the current distribution of the model [40]. Therefore, the dielectric behavior of the biological tissues is only associated with their resistance characteristics. In this case, the electrical current density (J) will have a linear relationship with the electrical field (E) in a volume conductor.

### *Anisotropic Electrical Conductivity*

The electrical conductivity of the brain tissues is anisotropic in real situations, and it can be approximated with a 3 × 3 symmetric tensor. However, for simplicity, the electrical conductivity of the brain tissues can be considered isotropic where the 3 × 3 tensor is converted to a scalar quantity. In this study, the average conductivity of each of the brain tissues was assumed, based on the information detailed in Table 1.

**Table 1.** Isotropic Conductivity Assignment

| | Brain Tissue | Electrical Conductivity (S. m-1) | Ref |
|---|---|---|---|
| 1 | Scalp | 0.43 | [36] |
| 2 | Skull | 0.015 | [37] |
| 3 | CSF | 1.79 | [38] |
| 4 | Gray Matter | 0.32 | [39] |
| 5 | White Matter | 0.15 | [40] |
| 6 | Electrodes | 1.4 | [36] |
| 7 | Gel | 0.43 | Conductivity of Scalp |

In a study conducted by Shahid et al. [21], various methods of measuring anisotropy were examined and compared in terms of accuracy. They found that the equivalent isotropic trace algorithm [1] had the highest accuracy for the estimation of the anisotropic feature of the brain tissues. Therefore, we applied this method in our study. In this method, the anisotropic electrical conductivity of the brain tissues is related to diffusion tensor as follows:

$$\sigma = \frac{3\sigma_{ISO}}{trace\ (D)}\ D \qquad (1)$$

Where $trace\ (D) = (D_{xx} + D_{yy} + D_{zz})$, $D$, and $\sigma_{iso}$ are diffusion tensor, diffusion tensor vector, and isotropic conductivity, respectively.

In this study, the diffusion tensor was extracted from the DT images using the FSL software package. To this aim, first the FDT-FMRIB Diffusion Toolbox 3.0 of the FSL 5.0.7 was used to correct the distortions due to eddy currents and possible movement of the subject. Then, the local tensor information was obtained using the DTIFit from the same library. In the next step, the anisotropic conductivity of the white matter volume was measured using the equivalent isotropic trace algorithm (described above), which was implemented in the Matlab software (R2010b, MathWorks, Natick, MA). Subsequently, the measured conductivity values were mapped to the elements in the meshed head using a method described in the literature [41-43]. Finally, the brain current distribution was calculated using the numerical solution method through the COMSOL version 4.1.

### *Electrical Field Calculation*

In order to calculate the electrical field and the electrical current density produced in the head in the tDCS, the meshed 3D model was imported into the COMSOL software package, and electrical conductivities were added to each of the tissues based on Table 1. The cathode and anode electrode surfaces were connected to the ground and current source, respectively; accordingly, a 2 mA current passed through it, and the other external surfaces were isolated.

### *Effect of The Geometry And Anisotropy of White Matter*

In order to investigate the effect of geometry on the current distribution, two approaches can be considered. These approaches include: 1) comparison of a realistic head model to a spherical brain model and 2) comparison of a homogeneous realistic head model (i.e., all brain tissues initialized with same electrical conductivity) with an inhomogeneous realistic head model (i.e., each brain tissue initialized with its specific electrical conductivity) (Table 1). In this study, we utilized the second approach.

The electrical conductivity of the homogeneous brain model was measured based on the average electrical conductivity, taking into account the volume. Then, the current distribution was calculated for these two cases, and the results were compared using a non-parametric statistical test (Wilcoxon signed-rank test) . Furthermore, in order to investigate the effect of the white matter anisotropy on the change of the head current intensity and distribution, the current distribution was calculated assuming white matter anisotropy, and the results were then compared with the isotropic case using the Wilcoxon signed-rank test.

## Results

### *Effect of Geometry on the Change of the Brain Current Distribution*

Figure 5 presents the results of the calculation of the electrical field in each subject, including the two cases of inhomogeneous realistic head model (the second column) and homogeneous realistic head model (the third column). The quantitative investigation of the results by the Wilcoxon test showed that the subjects' geometry had a significant effect ($P<0.05$) on the change of the current distribution in the gray and white matters.

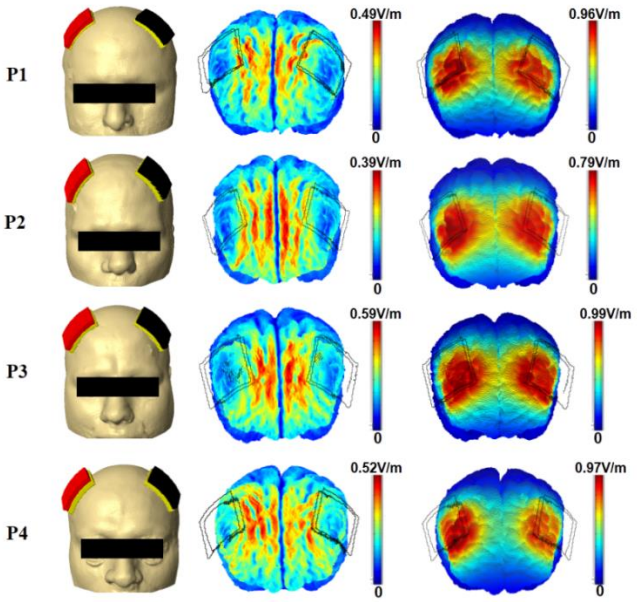


**Figure 5.** The effects of geometry on strength of induced electric field (EF). (a) Column 1: 3D releastic model of each patient with elocrodes placed on F3-F4 and Gel between electrode and skin. (b) Column 2: EF distributed on Gray matter surface of each patient based on inhomogeneous brain model (each brain tissue initialized with its specific electrical conductivity (Table.1)). (C) Column 3: EF distributed on Gray matter surface of each patient based on homogeneous brain model (All brain tissue initialized with same electrical conductivity).

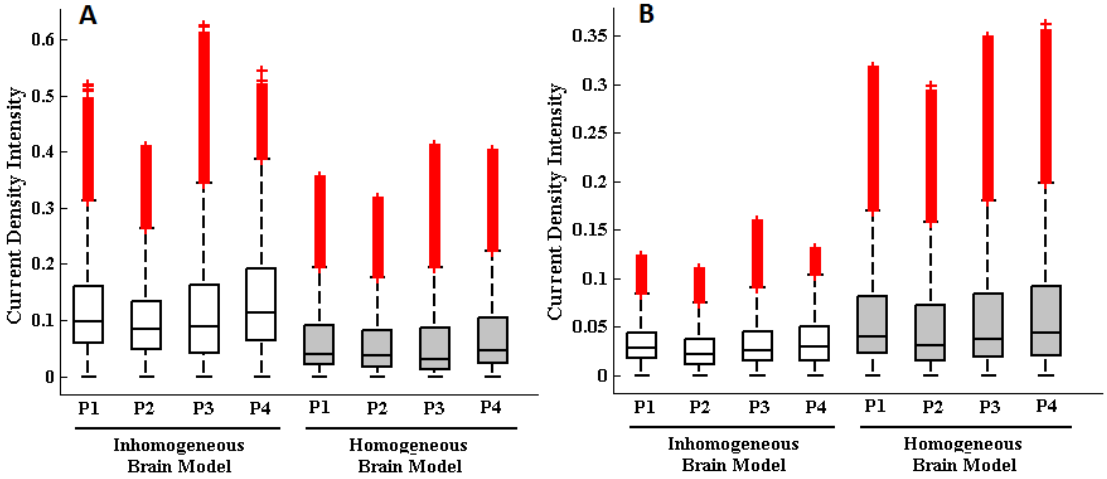


**Figure 6.** diagram A, is box plot for current density intensity distribution at Gray matter surface of four patients in two groups of inhomogeneous brain model and homogeneous brain model. Diagram B is box plot for current density intensity distribution at White matter surface of four patients in two groups of inhomogeneous brain model and homogeneous brain model. (Red lines are outliers which are more than 1.5 times of upper quartile)

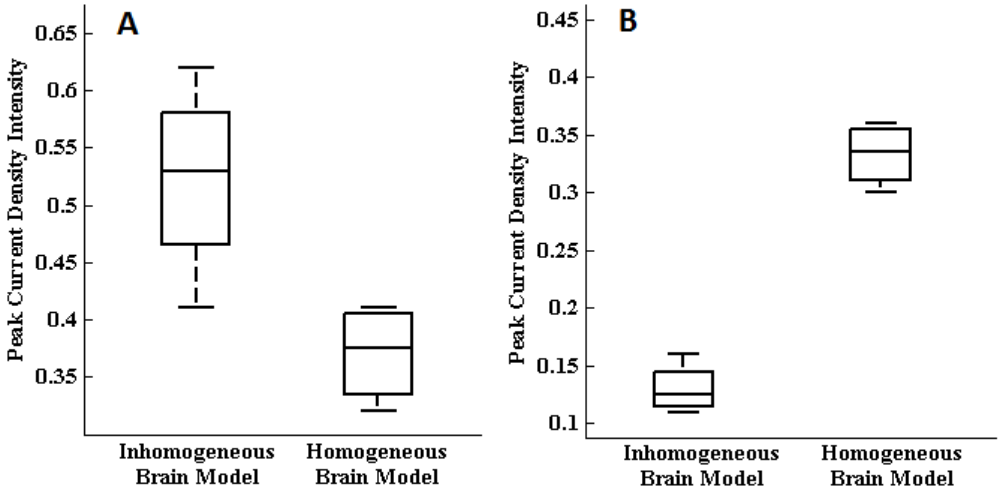


**Figure 7.** A. box plot of peak of current density intensity for 4 patients at Gray matter surface for inhomogeneous and homogeneous brain model. B. box plot of peak of current density intensity for 4 patients at White matter surface for inhomogeneous and homogeneous brain model.

**Table2.** Statistical data of peak of current density intensity at Gray and White matter surface for each two groups based on Figure 7.

| Groups | Tissues | Min | Max | Mean | Std Error | Std Deviation | Var |
|---|---|---|---|---|---|---|---|
| Inhomogeneous | GM | 0.41 | 0.62 | 0.5225 | 0.04329 | 0.08655 | 0.007 |
| Brain Model | WM | 0.11 | 0.16 | 0.13 | 0.0108 | 0.0216 | 0.000 |
| Homogeneous | GM | 0.32 | 0.41 | 0.37 | 0.02121 | 0.04243 | 0.002 |
| Brain Model | WM | 0.13 | 0.38 | 0.29 | 0.0558 | 0.11165 | 0.012 |

**Table3.** Statistical data of peak of current density intensity at Gray matter surface and under electrode for 4 inhomogeneous brain model.

| Tissue | Min | Max | Mean | Std Error | Std Deviation | Var |
|---|---|---|---|---|---|---|
| GM Surface | 0.41 | 0.62 | 0.5225 | 0.04328 | 0.08655 | 0.007 |
| Under Electrode | 0.34 | 0.47 | 0.4075 | 0.02686 | 0.05377 | 0.003 |

In order to further investigate this issue, the size of the current density in the gray and white matters of each of the subjects were measured, and the results are shown in Figure 6.

In addition, the maximum electrical current densities of the gray and white matters for the inhomogeneous and homogeneous cases for four subjects are shown in Figure 7. Furthermore, based on Figure 7, such statistical data as the maximum, minimum, mean, standard error, standard deviation, and variance for the peak current density intensities were calculated for each of the groups (Table 2).

Although the investigation of electrical current distribution in the gray matter is important, the

current distribution in the region of interest has even greater significance. In this study, the region of interest was located below the anode electrodes at the cortical layer. The maximum current density below the anode electrode and its statistical components are displayed in Figure 8 and Table 3.

### *Effect of Anisotropy on the Brain Electrical Current Distribution*

In order to investigate the effect of anisotropy on the changing of the current density intensity, the white matter anisotropy was added to each of the models. The results of the head current distribution, taking into account the effect of the white matter anisotropy, are demonstrated in Figure 9 (the third column). According to the results of the Wilcoxon test, the white matter anisotropy had a significant effect on the changing of the current distribution across the white matter ($P<0.05$); nevertheless, it did not have any significant effect across the gray matter ($P>0.05$). The sizes of the current density across the gray and white matters for each of the subjects are shown in Figure 10.

For further exploration, the statistical characteristics, such as the maximum, mean, variance, and standard error of the current density distributed across the gray and white matters were also evaluated (Table 4). In addition, the distribution of the maximum electrical current across the gray and white matters are illustrated in Figure 11 for the isotropic and anisotropic cases for the four subjects. Figure 12 displays the electrical current density distribution across the gray matter and below the anode electrode at the cortical layer for the anisotropic case for the four subjects.

Although the investigation of the effect of the geometry and anisotropy of the brain tissues on the gray and white matters is of special importance, the effect of such changes can also be very important from the cellular perspective. This is because the orientation of axonal or somatodendritic axis is a particularly important determinant of the polarizing effect of direct current to the electric field [44, 45].

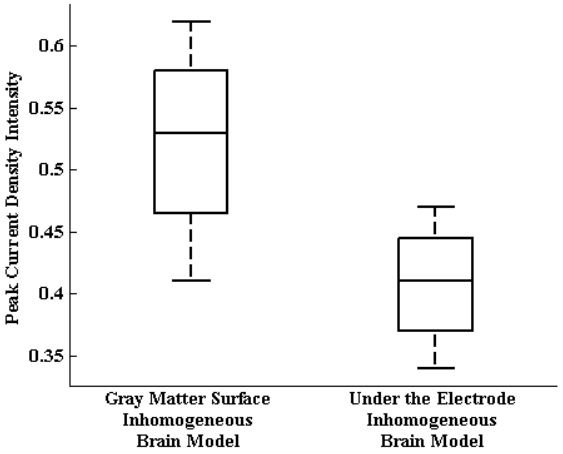


**Figure 8.** Box plot of peak of current density intensity for 4 patients at Gray matter surface and under the electrodes for inhomogeneous brain model.

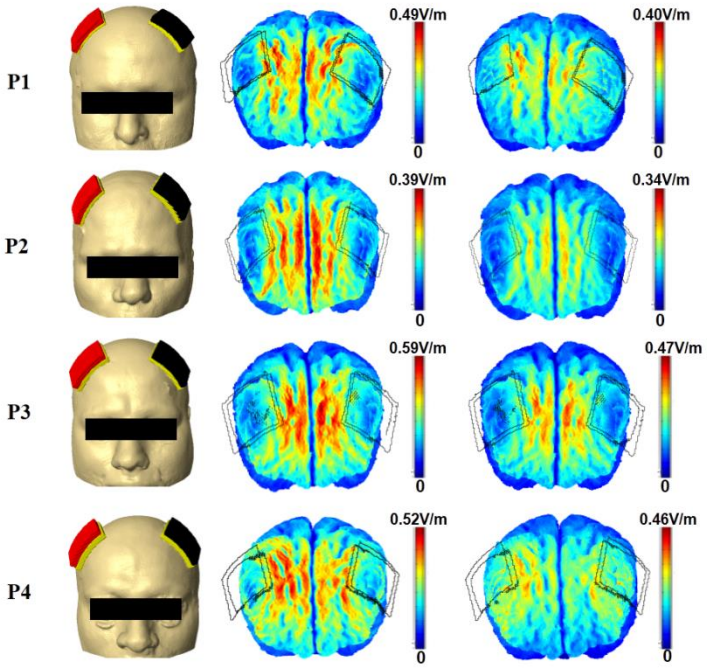


**Figure 9.** The effects of anisotropy on strength of induced electric field (EF). (a) Column 1: 3D realistic model of each patient with electrodes placed on F3-F4 and Gel between electrode and scalp. (b) Column 2: EF distributed on Gray matter surface of each patient for isotropic brain model. (c) Column 3: EF distributed on gray matter surface of each patient for anisotropic brain model.

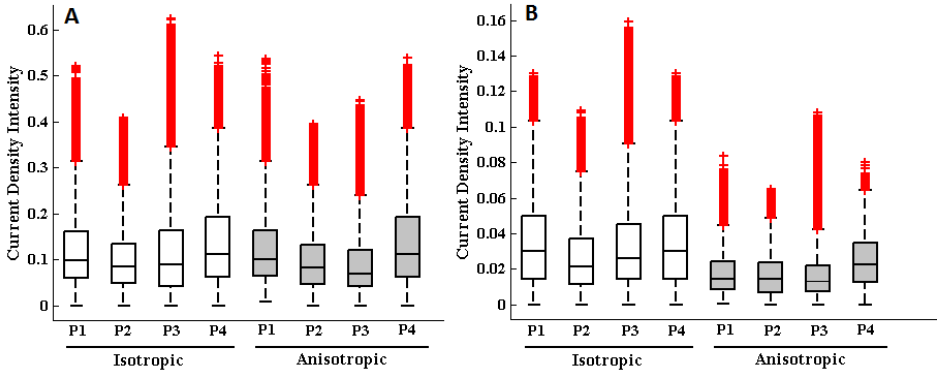


**Figure 10.** Diagram A, is box plot for current density intensity distribution at Gray matter surface of 4 patients in two groups of isotropic and anisotropic brain model. Diagram B is box plot for current density intensity distribution at White matter surface of 4 patients in two groups of isotropic and anisotropic brain model.

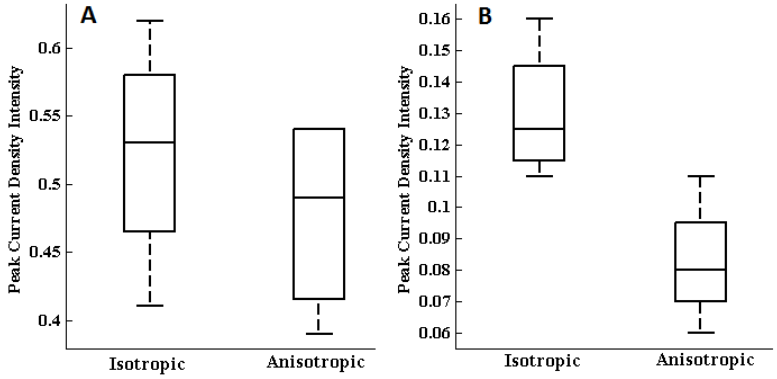


**Figure 11.** A. box plot of peak of current density intensity for 4 patients at Gray matter surface for isotropic and anisotropic brain model. B. box plot of peak of current density intensity for 4 patients at White matter surface for isotropic and anisotropic brain model.

**Table 4.** Statistical data of peak of current density intensity at Gray and White matter surface for isotropic and anisotropic brain model based on Figure 10.

| | Tissue | Min | Max | Mean | Std Error | Std Deviation | Var |
|---|---|---|---|---|---|---|---|
| Isotropic | GM | 0.41 | 0.62 | 0.5225 | 0.04328 | 0.08655 | 0.007 |
| | WM | 0.11 | 0.16 | 0.13 | 0.0108 | 0.0216 | 0.000 |
| Anisotropic | GM | 0.39 | 0.54 | 0.4775 | 0.0375 | 0.075 | 0.006 |

**Table 5.** The size of radial and tangential component and dominant component of current density for each subject at three points (the first point was the center of the anode electrode in the brain cortex, the second point was at the location of maximum electrical current and the third point was the center point of the two electrodes along the line connecting the electrodes centers). T: Tangential and R: Radial

| Subjects | Point 1 Intensity mA | Point 1 Direction T/R Dominant | Point 2 Intensity mA | Point 2Direction T/R Dominant | Point 3 Intensity mA | Point 3 Direction T/R Dominant |
|---|---|---|---|---|---|---|
| 1 | 0.27 | Tangential | 0.66 | Radial | 0.31 | Tangential |
| 2 | 0.35 | Radial | 0.44 | Tangential | 0.29 | Radial |
| 3 | 0.22 | Radial | 0.51 | Radial | 0.35 | Radial |
| 4 | 0.43 | Tangential | 0.49 | Tangential | 0.26 | Tangential |

The recent in vitro studies also reported that the neuronal segments that are oriented toward the stimulating anode were found to hyperpolarize, while the segments toward the cathode depolarized [38, 46, 47]. However, if the neuron is oriented perpendicular to the electric field, there will be no polarization effect. In order to investigate the effect of geometry and anisotropy on the creation of various types of excitability at the cellular level, three points were selected as candidates, and the sizes of the tangent and radial current density components were obtained for each of the points. The first point was the center of the anode electrode in the brain cortex, the second point was at the location of the maximum electrical current, and the third point was the center point of the two electrodes along the line connecting the electrode centers.

We assumed that the current density components measured at each point were applied to the cell axis of a neuron. Then, based on the modeling and physiological findings (as explained above), we supposed that the current density components

parallel to the neuronal axis increased the neuronal excitability, whereas the perpendicular components had no effect on excitability. The results of the sizes of the radial and tangent current density components for each of the subjects are demonstrated in Table 5.

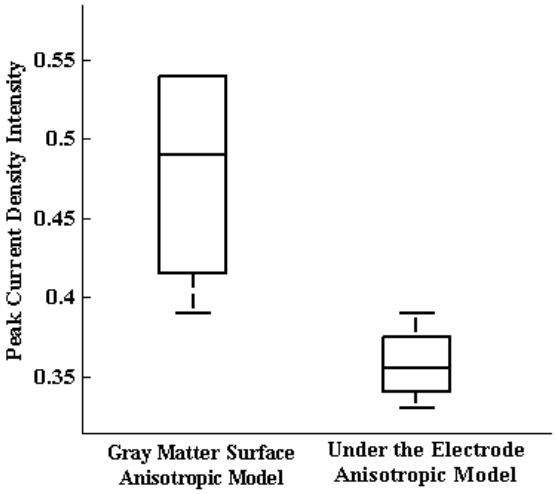


**Figure 12.** Box plot of peak of current density intensity for 4 patients at Gray matter surface and under the Anode electrode for anisotropic brain model.

## Discussion

The studies on tDCS are usually planned by assuming increased/decreased excitability under the anode/cathode electrode [48]. However, the recent studies have highlighted that the achievement of the classical "anodal- facilitatory/cathodal-inhibitory" effect of tDCS is far too simplistic [25]. The response variability and nonlinearity to tDCS arise from the fact that there are several factors, which are highly effective in shaping the tDCS outcome. These factors include the brain state, age, gender, brain geometrical structure, and specific electrical specifications of the brain tissue in each individual [17].

Out of these factors, individual geometry and brain tissue specifications play an important role in changing the size and direction of the distributed current during tDCS, which in turn can create different response to the same stimulation protocol. In the present study, we aimed to investigate the effect of the geometry and anisotropy of the brain tissues on the changing of the size and distribution of the brain electrical current during tDCS. To this aim, we utilized a realistic head current distribution modeling, incorporating MR-derived final element head modeling and DT images. The results were analyzed at the whole brain, below electrodes, and cellular levels for the cases of homogeneous, inhomogeneous, and anisotropic realistic head models.

### *Analysis of the Effect of Geometry*

The initial models of tDCS employed simplified geometries, such as point-like electrodes and concentric spheres, which could be solved analytically as well as numerically [28, 49]. The recent neuroimaging-based simulation studies have highlighted that the inter-individual differences in cranial and brain anatomy can influence the impact of tDCS by creating variability in the actual current received by the brain, even when the same electrical dose is administered [19, 50-52].

These findings are important in several ways. First, the earlier models fail to distinguish the individual differences between the healthy people and the impact of pathologic anatomy, such as skull defects and brain lesions [53], which can result in significant distortions in the current flow. In line with the recent studies, our results demonstrated that the geometry of the brain tissues had a significant effect on the changes of the electrical current intensity and distribution. In this regard, the brain tissue geometry affected the electrical current intensity in the gray and white matter surfaces by as much as 29% and 55%, respectively.

Furthermore, in the analytical models, the head current distribution was obtained while the maximum current density was below the electrodes. However, the results of those simple approaches are inconsistent with the new MRI-derived modeling studies, which suggest broad neuronal activation with peak brain modulation potentially between electrodes [27, 30, 48, 54, 55].

This finding is also in line with our result in which the examination of the current distribution showed that in addition to a large difference between the maximum electrical field of the inhomogeneous and homogeneous models. Whereas the maximum and accumulation of current was placed between the two electrodes for the inhomogeneous model, in the homogeneous models, it was located below the electrodes, increasing the accuracy of the model and applying the effect of real geometry.

This is due to the effect of asymmetrical geometry and also the small distance between the two electrodes and the consequent increase of the currents passing through the skin. In addition, it should be noted that even if a different geometry does not lead to a change in the size of the current, it may change its direction and dispersion, and consequently stimulate the cells quite differently.

### *Analysis of White Matter Anisotropy Effect*

The pyramidal and thalamocortical projection fiber tracts in the white matter can shape the orientation of the current flow more parallel to the main direction of the white matter fiber bundles [52]. The recent modeling studies have also highlighted the impact of individual differences in

terms of the anatomical fiber connectivity between the brain regions on the current distribution during tDCS [21, 37, 56, 57].

In this study, the examination of the effect of the white matter anisotropy on the change of electrical current demonstrated a significant difference between the values obtained from the measurements of the isotropic and anisotropic cases on the white matter. Anisotropy affected the electrical current intensity on the surface of the gray and white matters by as much as 8% and 36%, respectively. In this respect, our results are in line with the findings obtained in several studies [58-60]. However, instead of using fixed anisotropy ratios, we utilized the equivalent isotropic trace algorithm, which was more accurate for the estimation of the anisotropic feature of the brain tissues [21].

Based on the size, mean, and variance of the electrical current density measured across the gray matter and below the anode electrode, it could be concluded that the homogeneity of current distribution below the electrodes was the result of the existence of large plate electrodes. This finding was significant from two perspectives. First, for the isotropic case, the homogeneous distribution of the current below the anode electrodes prevented from different and uncontrolled stimulations of each part below the electrode. Second, although the application of anisotropy was expected to lead to an increase in the current dispersion below the electrodes, the results indicated that the homogeneity below the electrodes was well-maintained.

The stability of the current distribution homogeneity below the electrodes might be due to the large size of electrodes and also the low effect of white matter anisotropy on the current distribution across the gray matter. However, the differing geometry and anisotropy of the various brain tissues caused the maximum electrical current to occur at a point between the electrodes. Accordingly, the current distribution in locations other than below the electrodes was highly dispersed. This is an important issue, as the stimulation of points other than the region of interest might affect the tDCS results.

### *Analysis of the Effect of Transcranial Direct Current Stimulation from the Cellular Perspective*

The results obtained from the surface of the gray and white matters and the region of interest indicated the considerable effects of geometry and anisotropy on the magnitude and distribution of the head current. Moreover, it is very important to investigate the rate of the effect of these factors from a cellular perspective. This is because the orientation of axonal or somatodendritic axis is a particularly important determinant of the polarizing effect of the direct current electric field [44, 45]. The axon terminals are thought to be two to three times more susceptible than somas to tDCS-induced polarization.

In addition, the axonal orientation could determine whether the DC field is excitatory or inhibitory, whereas dendritic orientation could affect the magnitude but not the direction of DC resulting effects [61, 62]. The modeling of the head current distribution revealed that the dominant direction of the applied electrical current was tangential between the two electrodes and radial below the electrodes.

In addition, the physiological investigations have demonstrated that the primary effect of tDCS is caused by a change in the potential of the pyramidal cells in layer five of the brain cortex. Furthermore, these investigations have revealed that the currents parallel to the cell axis have a much greater effect on the increase of neuronal excitability than the currents perpendicular to it [61, 63].

The recent in vitro studies also reported that the neuronal segments that are oriented toward the stimulating anode hyperpolarize, while the segments toward the cathode depolarize [38, 46, 47]. However, if the neuron is oriented perpendicular to the electric field, there will be no polarization effect. Nevertheless, the existing methods are not yet able to specify the physiological features of the brain cortex, such as cell alignment, size, and structure at the cellular level for each person in a noninvasive way. Therefore, an investigation of the role of the direction and structure of the brain cortex cells can only be considered and discussed approximately and relatively.

In the present study, in order to obtain insights on the effect of tangential and radial components of the electrical current at the cellular level, three points were selected for analysis. The first point was the center of the anode electrode in the brain cortex, the second point was at the location of maximum electrical current, and the third point was the center point of the two electrodes along the line connecting the electrode centers. The magnitude of the normal current as well as radial and tangential components were obtained at these points.

We assumed that the current density components measured at each point were applied to the cell axis of a neuron. Then, based on the modeling and physiological findings, we supposed that the current density components parallel to the neuronal axis increased the neuronal excitability, whereas the perpendicular components had no effect in this regard. For example, for subject 1 (based on Table 5), the dominant current density component at point 1 was tangential, whereas it was radial for subject 2.

Regarding this, it could be concluded that the excitability of neuron at point 1 for subject 1 would increase, while this condition remained unchanged for subject 2 at this point .However, even though these points were carefully located and measured in

each subject, the magnitude of the current and its radial and tangential components differed greatly. This difference was to the point that for one subject, the point below the anode electrode had a totally dominant tangential component, while for another, the radial component was dominant.

This is an important issue signifying the difficulty of identifying the exact causes of cell excitation, since the factor causing excitation in one subject does not do so in another. In addition, from the cellular perspective, the differences in excitability lead to different synaptic connections, which is important for the long lasting effect of tDCS.

**Limitations and Future Directions**

Given the high variability in gyri and sulci patterns between individuals [64], it is not simple to report computational results. The majority of the studies have reported their modeling results graphically on 3D brain surfaces, which give a clear idea concerning the distribution of the electric fields. Nonetheless, it is difficult to perform a comparative analysis of different individuals by means of these approaches [35]. In this regard, the surface registration approach [65], which is based on mapping each point on the surface of one brain to that of another, may give us better insight for the analysis of inter-subject variations in tDCS electric fields and can be considered in future studies.

In the present study, the head geometry was segmented into five sections to investigate the effect of electrical stimulation in the brain. However, other studies [66, 67] have shown that the fat and muscles between the scalp and skull can affect the current density in the gray and white matters. Furthermore, in a study [68], the internal tissues of the brain was segmented into forty constituent sections, which enhanced the accuracy of the calculations of current distribution modeling and could be considered in future studies.

Although the use of the DT images to investigate the effect of brain tissue anisotropy has some advantages, it also has some limitations. These limitations include the assumption of Gaussian diffusion of water molecules in each voxel, the approximation of diffusion tensor in a voxel with high size [69] (which is very high in comparison with the bundle size), and the high error of this method in the estimation of the intersecting bundle direction. Therefore, it is not clear whether this method can accurately estimate the anisotropic features of the brain tissues, specifically for the modeling approach in tDCS.

To improve the accuracy of the tensor information and conductivity estimates, one could employ the model-free reconstruction methods, such as Q-ball [70] with diffusion spectrum imaging [71], which would allow multiple current flow directions within a single voxel. Alternatively, diffusion data may be acquired using high-resolution diffusion imaging scheme [72]. In addition, the complexity of tDCS, which makes it time-consuming, and the low accuracy of modeling methods in some cases have made it difficult to use this method in clinical applications. Therefore, the newer methods of conductivity and current density imaging, such as magnetic resonance electrical impedance tomography, may be more appropriate in this regard [73, 74].

## Conclusion

The tDCS has been applied in a wide range of neurological disorders due to the lack of any reports on its adverse effects. However, the response variability between the subjects in a similar test is regarded as one of the main challenges of this therapeutic method. In this study, we utilized the head current distribution modeling using MR images based on numerical solutions in order to investigate the effects of tDCS (taking into account the asymmetrical geometry and anisotropy of the brain tissues).

Based on the results of the models, it was shown that the geometry and anisotropy of each person's brain tissues had a significant role in changing the electrical current intensity. As the models revealed, the geometry of the brain tissues affected the electrical current intensity across the gray and white matters by as much as 29% and 55%, respectively. In addition, taking into account the anisotropy of the white matter led to 8% and 36% changes in the current density across the gray and white matters, respectively.

As the findings of the present study indicated, different geometry led to changes in the head current distribution so that the distribution was meaningfully different from one person to another. In addition, the white matter anisotropy of the brain tissues was found to affect the size and dispersion of the electrical current, mostly on the inside of the brain, and did not significantly influence the CDI on the gray matter surface. Although the dispersion in the whole brain increased as a result of the anisotropy of the white matter, the dispersion did not lead to any significant effect below the electrodes probably because of the employment of large electrodes.

Considering the difference between the rate of the maximum current and the electrical current distribution in one person with respect to another, these differences were of higher significance from a cellular point of view. Although the size of the electrical current had very important effects on the cellular excitability, the direction of the electrical current was also regarded as having a major effect on cellular excitability.

## References


1. Batsikadze G, Moliadze V, Paulus W, Kuo MF, Nitsche MA. Partially non-linear stimulation intensity-dependent effects of direct current stimulation on motor cortex excitability in humans. The Journal of physiology. 2013 Apr 1;591(7):1987-2000. DOI: 10.1113/jphysiol.2012.249730.
2. Monte-Silva K, Kuo MF, Hessenthaler S, Fresnoza S, Liebetanz D, Paulus W, et al. Induction of late LTP-like plasticity in the human motor cortex by repeated non-invasive brain stimulation. Brain stimulation. 2013 May 31;6(3):424-32. DOI: 10.1016/j.brs.2012.04.011.
3. Nitsche MA, Doemkes S, Karakoese T, Antal A, Liebetanz D, Lang N, et al. Shaping the effects of transcranial direct current stimulation of the human motor cortex. Journal of neurophysiology. 2007 Apr 1;97(4):3109-17. DOI: 10.1152/jn.01312.2006.
4. Kuo HI, Bikson M, Datta A, Minhas P, Paulus W, Kuo MF, et al. Comparing cortical plasticity induced by conventional and high-definition 4× 1 ring tDCS: a neurophysiological study. Brain stimulation. 2013 Jul 31;6(4):644-8. DOI: 10.1016/j.brs.2012.09.010.
5. Ho KA, Taylor JL, Chew T, Gálvez V, Alonzo A, Bai S, et al. The effect of transcranial direct current stimulation (tDCS) electrode size and current intensity on motor cortical excitability: evidence from single and repeated sessions. Brain stimulation. 2016 Feb 29;9(1):1-7. DOI: 10.1016/j.brs.2015.08.003.
6. Ferrucci R, Mameli F, Guidi I, Mrakic-Sposta S, Vergari M, Marceglia SE, et al. Transcranial direct current stimulation improves recognition memory in Alzheimer disease. Neurology. 2008 Aug 12;71(7):493-8. DOI: 10.1212/01.wnl.0000317060.43722.a3.
7. Marceglia S, Mrakic-Sposta S, Rosa M, Ferrucci R, Mameli F, Vergari M, et al. Transcranial direct current stimulation modulates cortical neuronal activity in Alzheimer's disease. Frontiers in neuroscience. 2016;10. DOI: 10.3389/fnins.2016.00134.
8. Doruk D, Gray Z, Bravo GL, Pascual-Leone A, Fregni F. Effects of tDCS on executive function in Parkinson's disease. Neuroscience letters. 2014 Oct 17; 582:27-31. DOI: 10.1016/j.neulet.2014.08.043.
9. Fregni F, Boggio PS, Santos MC, Lima M, Vieira AL, Rigonatti SP, et al. Noninvasive cortical stimulation with transcranial direct current stimulation in Parkinson's disease. Movement disorders. 2006 Oct 1;21(10):1693-702. DOI: 10.1002/mds.21012.
10. Hummel FC, Cohen LG. Non-invasive brain stimulation: a new strategy to improve neurorehabilitation after stroke?. The Lancet Neurology. 2006 Aug 31;5(8):708-12. DOI: 10.1016/S1474-4422(06)70525-7.
11. Boggio PS, Nunes A, Rigonatti SP, Nitsche MA, Pascual-Leone A, Fregni F. Repeated sessions of noninvasive brain DC stimulation is associated with motor function improvement in stroke patients. Restorative neurology and neuroscience. 2007 Jan 1;25(2):123-9.
12. Boggio PS, Rigonatti SP, Ribeiro RB, Myczkowski ML, Nitsche MA, Pascual-Leone A, et al. A randomized, double-blind clinical trial on the efficacy of cortical direct current stimulation for the treatment of major depression. International Journal of Neuropsychopharmacology. 2008 Mar 1;11(2):249-54. DOI: 10.1017/S1461145707007833.
13. Fregni F, Boggio PS, Nitsche MA, Marcolin MA, Rigonatti SP, Pascual-Leone A. Treatment of major depression with transcranial direct current stimulation. Bipolar disorders. 2006 Apr 1;8(2):203-4. DOI: 10.1111/j.1399-5618.2006.00291.x.
14. Fregni F, Freedman S, Pascual-Leone A. Recent advances in the treatment of chronic pain with non-invasive brain stimulation techniques. The Lancet Neurology. 2007 Feb 28;6(2):188-91. DOI: 10.1016/S1474-4422(07)70032-7.
15. Fregni F, Liguori P, Fecteau S, Nitsche MA, Pascual-Leone A, Boggio PS. Cortical stimulation of the prefrontal cortex with transcranial direct current stimulation reduces cue-provoked smoking craving: a randomized, sham-controlled study. Journal of Clinical Psychiatry. 2008 Jan 1;69(1):32-40.
16. Fregni F, Orsati F, Pedrosa W, Fecteau S, Tome FA, Nitsche MA, et al. Transcranial direct current stimulation of the prefrontal cortex modulates the desire for specific foods. Appetite. 2008 Jul 31;51(1):34-41. DOI: 10.1016/j.appet.2007.09.016.
17. Krause B, Kadosh RC. Not all brains are created equal: the relevance of individual differences in responsiveness to transcranial electrical stimulation. Frontiers in systems neuroscience. 2014;8. DOI: 10.3389/fnsys.2014.00025.
18. Terney D, Antal A, Paulus W. Towards unravelling task-related modulations of neuroplastic changes induced in the human motor cortex. Brain Stimulation. 2008 Jul 31;1(3):255-6. DOI: 10.1111/j.1460-9568.2007.05896.x.
19. Bikson M, Rahman A, Datta A. Computational models of transcranial direct current stimulation. Clinical EEG and Neuroscience. 2012 Jul;43(3):176-83. DOI: 10.1177/1550059412445138.
20. Truong DQ, Magerowski G, Blackburn GL, Bikson M, Alonso-Alonso M. Computational modeling of transcranial direct current stimulation (tDCS) in obesity: impact of head fat and dose guidelines. NeuroImage: Clinical. 2013 Dec 31;2: 759-66. DOI: 10.1016/j.nicl.2013.05.011.
21. Shahid S, Wen P, Ahfock T. Numerical investigation of white matter anisotropic conductivity in defining current distribution under tDCS. Computer methods and programs in biomedicine. 2013 Jan 31;109(1):48-64. DOI: 10.1016/j.cmpb.2012.09.001.
22. Wiethoff S, Hamada M, Rothwell JC. Variability in response to transcranial direct current stimulation of the motor cortex. Brain stimulation. 2014 Jun 30;7(3):468-75. DOI: 10.1016/j.brs.2014.02.003.
23. López-Alonso V, Cheeran B, Río-Rodríguez D, Fernández-del-Olmo M. Inter-individual variability in response to non-invasive brain stimulation paradigms. Brain stimulation. 2014 Jun 30;7(3):372-80. DOI: 10.1016/j.brs.2014.02.004.
24. Dyke K, Kim S, Jackson GM, Jackson SR. Intra-subject consistency and reliability of response following 2 mA transcranial direct current stimulation. Brain

stimulation. 2016 Dec 31;9(6):819-25. DOI: 10.1016/j.brs.2016.06.052.
25. Jacobson L, Koslowsky M, Lavidor M. tDCS polarity effects in motor and cognitive domains: a meta-analytical review. Experimental brain research. 2012 Jan 1;216(1):1-0. DOI: 10.1007/s00221-011-2891-9.
26. Dmochowski JP, Bikson M, Datta A, Richardson J, Fridriksson J, Parra LC. On the role of electric field orientation in optimal design of transcranial current stimulation. InEngineering in Medicine and Biology Society (EMBC), 2012 Annual International Conference of the IEEE 2012 Aug 28 (pp. 6426-6429). IEEE.
27. Datta A, Bansal V, Diaz J, Patel J, Reato D, Bikson M. Gyri-precise head model of transcranial direct current stimulation: improved spatial focality using a ring electrode versus conventional rectangular pad. Brain stimulation. 2009 Oct 31;2(4):201-7. DOI: 10.1016/j.brs.2009.03.005.
28. Rush S, Driscoll DA. Current distribution in the brain from surface electrodes. Anesthesia & Analgesia. 1968 Nov 1;47(6):717-23.
29. Ruffini G, Wendling F, Merlet I, Molaee-Ardekani B, Mekonnen A, Salvador R, et al. Transcranial current brain stimulation (tCS): models and technologies. IEEE Transactions on Neural Systems and Rehabilitation Engineering. 2013 May;21(3):333-45. DOI: 10.1109/TNSRE.2012.2200046.
30. Salvador R, Mekonnen A, Ruffini G, Miranda PC. Modeling the electric field induced in a high resolution realistic head model during transcranial current stimulation. InEngineering in Medicine and Biology Society (EMBC), 2010 Annual International Conference of the IEEE 2010 Aug 31 (pp. 2073-2076). IEEE. DOI: 10.1109/IEMBS.2010.5626315.
31. Suh HS, Lee WH, Cho YS, Kim JH, Kim TS. Reduced spatial focality of electrical field in tDCS with ring electrodes due to tissue anisotropy. InEngineering in Medicine and Biology Society (EMBC), 2010 Annual International Conference of the IEEE 2010 Aug 31 (pp. 2053-2056). IEEE. DOI: 10.1109/IEMBS.2010.5626502.
32. Opitz A, Paulus W, Will S, Antunes A, Thielscher A. Determinants of the electric field during transcranial direct current stimulation. Neuroimage. 2015 Apr 1;109:140-50. DOI: 10.1016/j.neuroimage.2015.01.033.
33. Halko MA, Datta A, Plow EB, Scaturro J, Bikson M, Merabet LB. Neuroplastic changes following rehabilitative training correlate with regional electrical field induced with tDCS. Neuroimage. 2011 Aug 1;57(3):885-91. DOI: 10.1016/j.neuroimage.2011.05.026.
34. Arlotti M, Rahman A, Minhas P, Bikson M. Axon terminal polarization induced by weak uniform DC electric fields: a modeling study. InEngineering in Medicine and Biology Society (EMBC), 2012 Annual International Conference of the IEEE 2012 Aug 28 (pp. 4575-4578). IEEE. DOI: 10.1109/EMBC.2012.6346985.
35. Laakso I, Tanaka S, Koyama S, De Santis V, Hirata A. Inter-subject variability in electric fields of motor cortical tDCS. Brain stimulation. 2015 Oct 31;8(5):906-13. DOI: 10.1016/j.brs.2015.05.002.
36. Shahid SS, Bikson M, Salman H, Wen P, Ahfock T. The value and cost of complexity in predictive modelling: role of tissue anisotropic conductivity and fibre tracts in neuromodulation. Journal of neural engineering. 2014 Apr 16;11(3):036002. DOI: 10.1088/1741-2560/11/3/036002.
37. Suh HS, Lee WH, Kim TS. Influence of anisotropic conductivity in the skull and white matter on transcranial direct current stimulation via an anatomically realistic finite element head model. Physics in Medicine and Biology. 2012 Oct 9;57(21):6961. DOI: 10.1088/0031-9155/57/21/6961.
38. Metwally MK, Han SM, Kim TS. The effect of tissue anisotropy on the radial and tangential components of the electric field in transcranial direct current stimulation. Medical & biological engineering & computing. 2015 Oct 1;53(10):1085-101. DOI: 10.1007/s11517-015-1301-z.
39. Huang Y, Dmochowski JP, Su Y, Datta A, Rorden C, Parra LC. Automated MRI segmentation for individualized modeling of current flow in the human head. Journal of neural engineering. 2013 Oct 8;10(6):066004. DOI: 10.1088/1741-2560/10/6/066004.
40. Plonsey R, Heppner DB. Considerations of quasi-stationarity in electrophysiological systems. Bulletin of mathematical Biology. 1967 Dec 1;29(4):657-64.
41. Miranda PC, Pajevic S, Pierpoali C, Hallett M, Basser P. The distribution of currents induced in the brain by magnetic stimulation: a finite element analysis incorporating DT-MRI-derived conductivity data. InProceedings of the International Society for Magnetic Resonance in Medicine 2001 (Vol. 9).
42. Kim S, Kim TS, Zhou Y, Singh M. Influence of conductivity tensors in the finite element model of the head on the forward solution of EEG. InNuclear Science Symposium Conference Record, 2001 IEEE 2001 (Vol. 4, pp. 1892-1896). IEEE. DOI: 10.1109/NSSMIC.2001.1009193.
43. Abascal JF, Arridge SR, Atkinson D, Horesh R, Fabrizi L, De Lucia M, et al. Use of anisotropic modelling in electrical impedance tomography; description of method and preliminary assessment of utility in imaging brain function in the adult human head. Neuroimage. 2008 Nov 1;43(2):258-68. DOI: 10.1016/j.neuroimage.2008.07.023.
44. Purpura DP, McMurtry JG. Intracellular activities and evoked potential changes during polarization of motor cortex. Journal of neurophysiology. 1965 Jan 1;28(1):166-85.
45. Gluckman BJ, Neel EJ, Netoff TI, Ditto WL, Spano ML, Schiff SJ. Electric field suppression of epileptiform activity in hippocampal slices. Journal of Neurophysiology. 1996 Dec 1;76(6):4202-5.
46. Radman T, Ramos RL, Brumberg JC, Bikson M. Role of cortical cell type and morphology in subthreshold and suprathreshold uniform electric field stimulation in vitro. Brain stimulation. 2009 Oct 31;2(4):215-28. DOI: 10.1016/j.brs.2009.03.007.
47. Rattay F. Analysis of models for external stimulation of axons. IEEE transactions on biomedical engineering. 1986 Oct(10):974-7. DOI: 10.1109/TBME.1986.325670.

48. Datta A, Truong D, Minhas P, Parra LC, Bikson M. Inter-individual variation during transcranial direct current stimulation and normalization of dose using MRI-derived computational models. Frontiers in psychiatry. 2012;3. DOI: 10.3389/fpsyt.2012.00091.
49. Ferdjallah M, Bostick FX, Barr RE. Potential and current density distributions of cranial electrotherapy stimulation (CES) in a four-concentric-spheres model. IEEE Transactions on Biomedical Engineering. 1996 Sep;43(9):939-43. DOI: 10.1109/10.532128.
50. Li LM, Uehara K, Hanakawa T. The contribution of interindividual factors to variability of response in transcranial direct current stimulation studies. Frontiers in cellular neuroscience. 2015;9. DOI: 10.3389/fncel.2015.00181.
51. Bikson M, Rahman A, Datta A, Fregni F, Merabet L. High-Resolution Modeling Assisted Design of Customized and Individualized Transcranial Direct Current Stimulation Protocols. Neuromodulation: Technology at the Neural Interface. 2012 Jul 1;15(4):306-15.
52. Wagner S, Rampersad SM, Aydin Ü, Vorwerk J, Oostendorp TF, Neuling T, et al. Investigation of tDCS volume conduction effects in a highly realistic head model. Journal of neural engineering. 2013 Dec 5;11(1):016002. DOI: 10.1088/1741-2560/11/1/016002.
53. Datta A, Baker JM, Bikson M, Fridriksson J. Individualized model predicts brain current flow during transcranial direct-current stimulation treatment in responsive stroke patient. Brain stimulation. 2011 Jul 31;4(3):169-74. DOI: 10.1016/j.brs.2010.11.001.
54. Lang N, Siebner HR, Ward NS, Lee L, Nitsche MA, Paulus W, et al. How does transcranial DC stimulation of the primary motor cortex alter regional neuronal activity in the human brain?. European Journal of Neuroscience. 2005 Jul 1;22(2):495-504. DOI: 10.1111/j.1460-9568.2005.04233.x.
55. Sadleir RJ, Vannorsdall TD, Schretlen DJ, Gordon B. Transcranial direct current stimulation (tDCS) in a realistic head model. Neuroimage. 2010 Jul 15;51(4):1310-8. DOI: 10.1016/j.neuroimage.2010.03.052.
56. Metwally MK, Cho YS, Park HJ, Kim TS. Investigation of the electric field components of tDCS via anisotropically conductive gyri-specific finite element head models. InEngineering in Medicine and Biology Society (EMBC), 2012 Annual International Conference of the IEEE 2012 Aug 28 (pp. 5514-5517). IEEE. DOI: 10.1109/EMBC.2012.6347243.
57. Russell MJ, Goodman T, Pierson R, Shepherd S, Wang Q, Groshong B, Wiley DF. Individual differences in transcranial electrical stimulation current density. Journal of biomedical research. 2013 Nov;27(6):495. DOI: 10.7555/JBR.27.20130074.
58. Holdefer RN, Sadleir R, Russell MJ. Predicted current densities in the brain during transcranial electrical stimulation. Clinical neurophysiology. 2006 Jun 30;117(6):1388-97. DOI: 10.1016/j.clinph.2006.02.020.
59. Oostendorp TF, Hengeveld YA, Wolters CH, Stinstra J, van Elswijk G, Stegeman DF. Modeling transcranial DC stimulation. InEngineering in Medicine and Biology Society, 2008. EMBS 2008. 30th Annual International Conference of the IEEE 2008 Aug 20 (pp. 4226-4229). IEEE. DOI: 10.1109/IEMBS.2008.4650142.
60. Suh HS, Kim SH, Lee WH, Kim TS. Realistic simulation of transcranial direct current stimulation via 3-D high-resolution finite element analysis: effect of tissue anisotropy. InEngineering in Medicine and Biology Society, 2009. EMBC 2009. Annual International Conference of the IEEE 2009 Sep 3 (pp. 638-641). IEEE. DOI: 10.1109/IEMBS.2009.5333686.
61. Rahman A, Reato D, Arlotti M, Gasca F, Datta A, Parra LC, et al. Cellular effects of acute direct current stimulation: somatic and synaptic terminal effects. The Journal of physiology. 2013 May 1;591(10):2563-78. DOI: 10.1113/jphysiol.2012.247171.
62. Kabakov AY, Muller PA, Pascual-Leone A, Jensen FE, Rotenberg A. Contribution of axonal orientation to pathway-dependent modulation of excitatory transmission by direct current stimulation in isolated rat hippocampus. Journal of neurophysiology. 2012 Apr 1;107(7):1881-9. DOI: 10.1152/jn.00715.2011.
63. Bikson M, Inoue M, Akiyama H, Deans JK, Fox JE, Miyakawa H, et al. Effects of uniform extracellular DC electric fields on excitability in rat hippocampal slices in vitro. The Journal of physiology. 2004 May 1;557(1):175-90. DOI: 10.1113/jphysiol.2003.055772.
64. Ono M, Kubik S, Abernathey CD. Atlas of the cerebral sulci. Tps; 1990.
65. Fischl B, Sereno MI, Tootell RB, Dale AM. High-resolution intersubject averaging and a coordinate system for the cortical surface. Human brain mapping. 1999 Jan 1;8(4):272-84.
66. Shahid S, Wen P, Ahfock T. Effect of fat and muscle tissue conductivity on cortical currents-a tDCS study. InComplex Medical Engineering (CME), 2011 IEEE/ICME International Conference on 2011 May 22 (pp. 211-215). IEEE. DOI: 10.1109/ICCME.2011.5876735.
67. Truong DQ, Magerowski G, Pascual-Leone A, Alonso-Alonso M, Bikson M. Finite element study of skin and fat delineation in an obese subject for transcranial direct current stimulation. InEngineering in Medicine and Biology Society (EMBC), 2012 Annual International Conference of the IEEE 2012 Aug 28 (pp. 6587-6590). IEEE. DOI: 10.1109/EMBC.2012.6347504.
68. Parazzini M, Fiocchi S, Rossi E, Paglialonga A, Ravazzani P. Transcranial direct current stimulation: estimation of the electric field and of the current density in an anatomical human head model. IEEE Transactions on Biomedical Engineering. 2011 Jun;58(6):1773-80. DOI: 10.1109/TBME.2011.2116019.
69. Le Bihan D, Mangin JF, Poupon C, Clark CA, Pappata S, Molko N, et al. Diffusion tensor imaging: concepts and applications. Journal of magnetic resonance imaging. 2001 Apr 1;13(4):534-46.

70. D.S. Tuch, Q-ball imaging, Magnetic resonance in medicine, 52 (2004) 1358-1372.
71. Wedeen VJ, Wang RP, Schmahmann JD, Benner T, Tseng WY, Dai G, et al. Diffusion spectrum magnetic resonance imaging (DSI) tractography of crossing fibers. Neuroimage. 2008 Jul 15;41(4):1267-77. DOI: 10.1016/j.neuroimage.2008.03.036.
72. Tuch DS, Reese TG, Wiegell MR, Makris N, Belliveau JW, Wedeen VJ. High angular resolution diffusion imaging reveals intravoxel white matter fiber heterogeneity. Magnetic resonance in medicine. 2002 Oct 1;48(4):577-82. DOI: 10.1002/mrm.10268.
73. Jog MV, Smith RX, Jann K, Dunn W, Lafon B, Truong D, et al. In-vivo imaging of magnetic fields induced by transcranial direct current stimulation (tDCS) in human brain using MRI. Scientific reports. 2016;6. DOI: 10.1038/srep34385.
74. Kwon OI, Sajib SZ, Sersa I, Oh TI, Jeong WC, Kim HJ, et al. Current Density Imaging during Transcranial Direct Current Stimulation (tDCS) using DT-MRI and MREIT: Algorithm Development and Numerical Simulations. IEEE Trans. on Biomedical Engineering. 2015;22. DOI: 10.1109/TBME.2015.2448555.